Journal of Hazardous Materials 497 (2025) 139725

Contents lists available at ScienceDirect

Journal of Hazardous Materials

journal homepage: www.elsevier.com/locate/jhazmat

Urban pollution impact assessment in six Lithuanian cities with a focus on road traffic emissions - integrated framework for environmental health studies

Simonas Kecorius [a,b,c,*], Leizel Madueño [d], Wolfram Birmili [e], Jakob Löndahl [f], Kristina Plauškaitė [a], Steigvilė Byčenkienė [a], Mario Lovrić [g,h], Valentino Petrić [h,i], Manuel Carranza-García [j], Manuel J. Jiménez-Navarro [j], María Martínez-Ballesteros [j], Magdalena Weiss [b,k], Otmar Schmid [k,l], Josef Cyrys [b], Annette Peters [b,m,n], Gaudentas Kecorius [o]

[a] Center for Physical Sciences and Technology (FTMC), Vilnius, Lithuania
[b] Institute of Epidemiology, Helmholtz Zentrum München—German Research Center for Environmental Health, Neuherberg, Germany
[c] Model-based Environmental Exposure Science, Faculty of Medicine, University of Augsburg, Augsburg, Germany
[d] Atmospheric Microphysics Department, Leibniz Institute for Tropospheric Research, Leipzig, Germany
[e] Department of Environmental Hygiene, German Environment Agency (Umweltbundesamt), Berlin, Germany
[f] Division of Ergonomics and Aerosol Technology, Department of Design Sciences, Lund University, Lund, Sweden
[g] Institute for Anthropological Research, Zagreb, Croatia
[h] Lisbon Council, Brussels, Belgium
[i] Ascalia d.o.o., Čakovec, Croatia
[j] Department of Computer Languages and Systems, University of Seville, Spain
[k] Institute of Lung Health and Immunity (LHI), Helmholtz Zentrum München, Neuherberg, Germany
[l] Comprehensive Pneumology Center (CPC-M), Member of the German Center for Lung Research (DZL), Munich, Germany
[m] Ludwig-Maximilians-University Munich, Munich, Germany
[n] Centre for Cardiovascular Research, Partner Site Munich Heart Alliance, Munich, Germany
[o] Private Researcher, Kupiškis, Lithuania

HIGHLIGHTS

- Integrated urban pollution impact assessment framework is presented.
- Pollution is affected by city size and diesel vehicle fraction.
- Vilnius has the highest pollution levels due to its size and traffic.
- Black carbon mass concentrations are similar to other European cities.
- Coarse mode particles determine respiratory tract deposition is some cities.

GRAPHICAL ABSTRACT

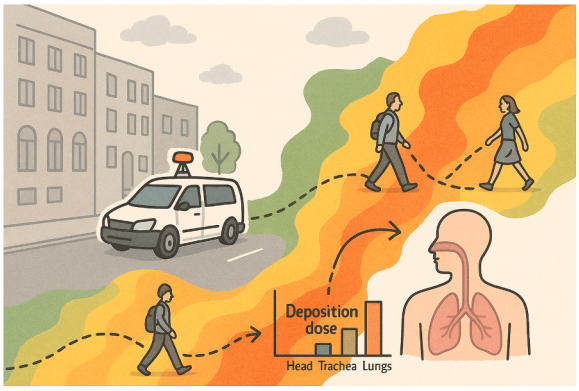

* Corresponding author at: Institute of Epidemiology, Helmholtz Zentrum München—German Research Center for Environmental Health, Neuherberg, Germany.
E-mail address: simonas.kecorius@helmholtz-munich.de (S. Kecorius).

https://doi.org/10.1016/j.jhazmat.2025.139725
Received 28 May 2025; Received in revised form 13 August 2025; Accepted 31 August 2025
Available online 2 September 2025

ARTICLE INFO

Keywords:
Lung deposited surface area
Particle number size distribution
Ultrafine particles
Exposure assessment
Urban pollution

ABSTRACT

An integrated framework is introduced and applied to assess the health impact of airborne pollution with greater physiological relevance, moving beyond conventional exposure metrics. Measured particle number size distribution data was integrated with a regional respiratory tract deposition fractions to estimate total and alveolar deposited particle surface area concentrations. Land use regression modeling, combined with randomized commuting patterns, enabled the evaluation of city-specific alveolar surface area deposition doses, providing new insight into localized average exposure and its implications for public health.

The results showed that although the mean street-level air pollution in Lithuania is higher than in other European cities, the urban background levels are on the same level. We found that the total respiratory deposited surface area concentration is up to 18-fold higher due to coarse particles, which also determines alveolar deposited particle surface area dose.

Our findings advocate for using integrated pollution assessments and region-specific policies rather than broad diesel vehicle-targeted bans. The proposed methodology is expected to enhance traditional exposure assessments by switching to lung deposited surface area, which can be further refined by incorporating daytime activity patterns, socio-economic status, and personal health conditions.

1. Introduction

Atmospheric air pollution, in particular combustion-generated particles, is associated with negative effects on human health, biological diversity, and the environment in general [28,51]. To tame the negative impacts of airborne pollution, the environmental status is constantly monitored through intensive field campaigns, as well as government operated long-term air quality monitoring networks focusing on regulated pollutants (e.g., particulate matter with aerodynamic diameters less than 10 (PM_{10}) and 2.5 ($PM_{2.5}$) micrometers, respectively; [72]). However, it has been recognized that besides commonly monitored PM_{10} and $PM_{2.5}$, other airborne pollutant metrics shall be incorporated in air pollution monitoring and regulation to further reduce health impacts [72]. There is growing evidence that aerosol particle number, surface area concentration, particle shape, mixing state, etc., are related to adverse health outcomes [11,28,6,70]. For example, multiple studies (e.g., [23,49,65]) showed that increased ultrafine particle (diameter $<$ 100 nm, UFP) number concentration can be related to respiratory mortality within one week after exposure. Schmid and Stoeger [64] suggested aerosol particle surface area concentration to be one of the most important lung-inflammation related parameters to be monitored by aerosol scientists.

Accordingly, some studies have also proposed lung deposited surface area concentration (LDSA) as a valuable means to evaluate links between exposure to airborne pollutants and associated health risks (e.g. [19,42,67]). From the exposure assessment perspective, the LDSA can identify material-specific nanotoxicity and provide information about particle interaction with the lungs [24,27,64]. The use of LDSA in environmental epidemiology can also be supported by studies in toxicology, where the negative effects of airborne pollutants are often investigated utilizing alveolar cell cultures, which replicate the cellular environment of the lungs' alveolar region—the site where gas exchange occurs and exhibits a relatively high particle deposition [71]. Once deposited in the alveolar region, aerosol particles can be translocated to other organs through transcytosis or alveolar macrophage-mediated transport, which can be causally linked to systemic health effects (e.g., [52,20,5]). In other words, it would be reasonable to expect that in health effects assessment studies, researchers would employ some respiratory tract deposited concentration/dose metric (e.g., number, surface, or mass). However, to the best of our knowledge, to date, there are no such examples – epidemiologists typically assess the health effects of airborne pollutants by utilizing information from ambient pollutant exposure assessment, which in turn heavily relies on standard metrics, such as PM_{10}, $PM_{2.5}$, total particle number concentration (PNC), and in more rare instances – size-resolved particle number concentration. Such an approach, although well established, does not provide a complete understanding of the dynamics between airborne pollutants and adverse health effects, which would otherwise be possible by the synergistic union between toxicological, exposure assessment, and epidemiological studies.

To facilitate the paradigm shift towards research that prioritizes deposited doses in specific lung regions over generic exposure assessment measurements, we developed land use regression (LUR) models for the respiratory tract (total and alveolar region) deposited particulate pollutant concentration by integrating mobile particle number size distribution (PNSD) measurements with a respiratory tract deposition model. The specific objectives of this study are to: (a) analyze high-resolution spatial and temporal measurements of equivalent (determined from light attenuation measurement using aethalometer) black carbon (eBC) and PNSD collected during a six-city mobile monitoring campaign in Northern Europe; (b) calculate deposited particle number and surface area concentrations in different respiratory regions by applying total respiratory and alveolar deposition efficiency curves to the measured PNSDs; and (c) from the developed LUR models evaluate alveolar deposited particulate surface area utilizing synthesized commuting paths for a population proxy. The presented methodology and initial findings in this study aim to enhance air pollution exposure assessment and provide epidemiologists with improved tools for evaluating health risks associated with airborne particulate matter.

2. Framework for segmented airway deposition-based pollution impact assessment

With the entry into force of Directive (EU) 2024/2881 on ambient air quality and cleaner air for Europe [17] on 10 December 2024, Member States have a two-year transposition period to incorporate its provisions into national law. This directive consolidates the former Directives 2004/107/EC and 2008/50/EC into a single legal framework and introduces more stringent limit values for key air pollutants. Specifically, the annual limit values for fine particulate matter and nitrogen dioxide are substantially lowered to levels that must be met by 1 January 2030. These revised thresholds are aligned with the [76] Air Quality Guidelines (WHO, 2021) to reflect the latest scientific evidence on health impacts. A central innovation of the directive is the establishment of monitoring "supersites," whose number and distribution—at least one per 100000 km^2 in large Member States and proportionate to population in all States. Moreover, these supersites are required to monitor emerging pollutants, including ultrafine particles via their particle number size distribution—parameters for which no EU limit values or mandatory monitoring existed previously.

In light of this, we propose the following framework to expand future health-related studies with a focus on airborne pollutants (Fig. 1), which was implemented in this work:

1. Determine which pollutant metrics are the most relevant for health studies based on evidence from toxicology studies. This step prioritizes the identification of pollutant physical-chemical properties that pose the greatest health risks, ensuring that future research targets the most impactful factors. While the new directive specifically mandates monitoring of PNSD and eBC at supersites, our work further focuses attention on eBC and LDSA (in several size ranges), as well as deposited dose. It is important to note that LDSA is not explicitly included in the new directive, but we consider it a crucial physiologically meaningful endpoint aligned with emerging environmental health research.
2. Adopt measurement instrumentation and techniques that are capable of capturing the most relevant pollutant metrics. This can be facilitated by including particle number size distribution measurements alongside long-established PM_{10} and $PM_{2.5}$ metrics. Given advancements in aerosol instrumentation, instruments able to measure size distribution (e.g., electric low-pressure impactors, mobility particle size spectrometers, non-contact electrical particle detectors, etc.) should be more often used in health risk assessments, supplementing well established metrics. The measurements shall be conducted covering long spatial and temporal domains (Fig. 1, A). In this work we have conducted repeated mobile measurements of PNSD and eBC in six different cities in Lithuania.
3. In addition to in-situ measurements, city-wide pollution maps are essential for supporting epidemiological studies of long-term effects of air pollution. To estimate spatial distributions of pollutants, various modeling approaches can be employed, including dispersion modeling and LUR (e.g., [60]). In this study, we applied LUR models that integrated pollutant measurements—extending beyond traditional $PM_{2.5}$ and PM_{10} metrics—with land-use variables such as traffic intensity, road types, and building density. This approach enabled the development of high-resolution pollution maps for six distinct urban environments (Fig. 1B).
4. To further expand the accuracy of pollution impact assessment on airborne populations, pollutant measurements shall be combined with respiratory deposition fraction studies (both laboratory and model development), as well as population mobility models representing actual population pollution impact (Fig. 1, C). This is because lung deposited dose and not the exposure concentration is responsible for toxicological effects. In this work, the respiratory deposition concentration and the deposited dose were calculated for different particle size ranges and metrics (Fig. 1, D). Such an integrated approach enhances health-assessment precision by accounting for how pollutants deposit in the respiratory system. It also allows to account for individual characteristics such as daytime activity patterns, socio-economic status, and physical parameters (gender, age, medical history).
5. Lastly, pollution mitigation strategies shall be tailored at decreasing the most relevant components of airborne pollutants, instead of relying on generic exposure parameters. This targeted focus ensures that mitigation efforts maximize health benefits with the least restrictive measures by mitigating the most harmful pollutant fractions.

3. Methods

3.1. Measurement domain

The intensive mobile measurement campaign took place in Lithuania in the summer of 2024 (June to August). The campaign was designed to be conducted in summer to limit different pollution source contribution (e.g., long-range transport of biomass burning products in spring and residential heating in cold months [7]. Regional atmospheric new particle formation (NPF) is known to contribute substantially to particle number concentrations and, in urban environments, may be misinterpreted as traffic-related pollution [32]. While NPF significantly affects particle number concentrations, the newly formed and subsequently grown particles do not contribute to equivalent black carbon mass. Moreover, analysis of the measured particle number size distributions revealed no evidence of nucleation events during the observation period. It can therefore be assumed that measured pollutant concentrations on the street entirely represent emissions from the vehicular fleet, with a minimal contribution from other pollution sources. The project's domain is shown in Fig. 2, and the measurement timelines are indicated in Table 1.

The mobile measurements were performed in the six largest cities in

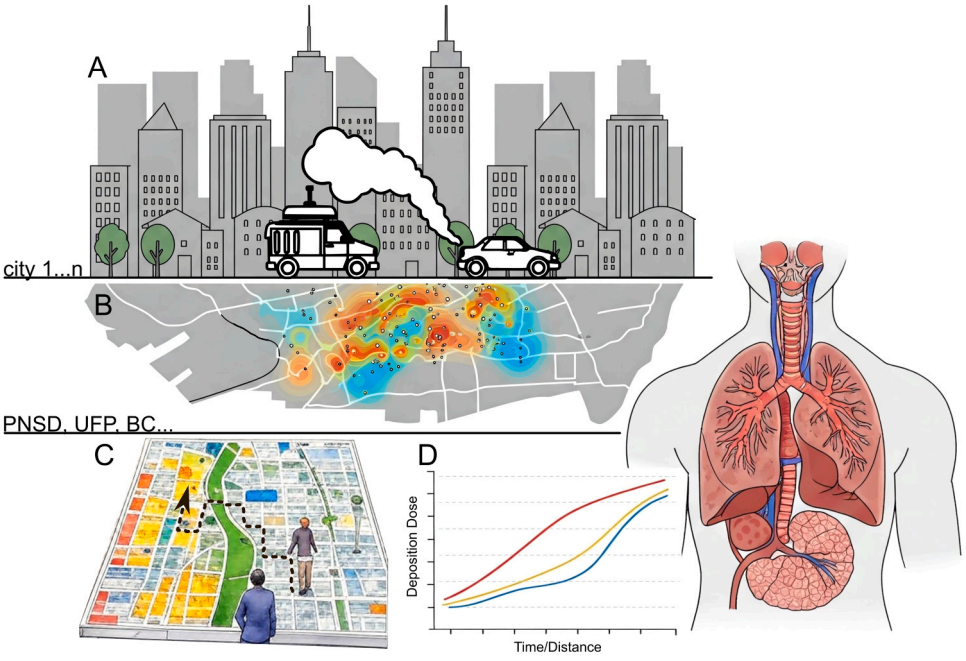

Fig. 1. Framework for integrated urban air pollution assessment based on mobile particle pollution measurements using toxicologically-derived pollution metrics (A), city-scale pollution modeling (B), commuting pattern simulation (C), and computation of lung deposited particulate matter parameters (D).

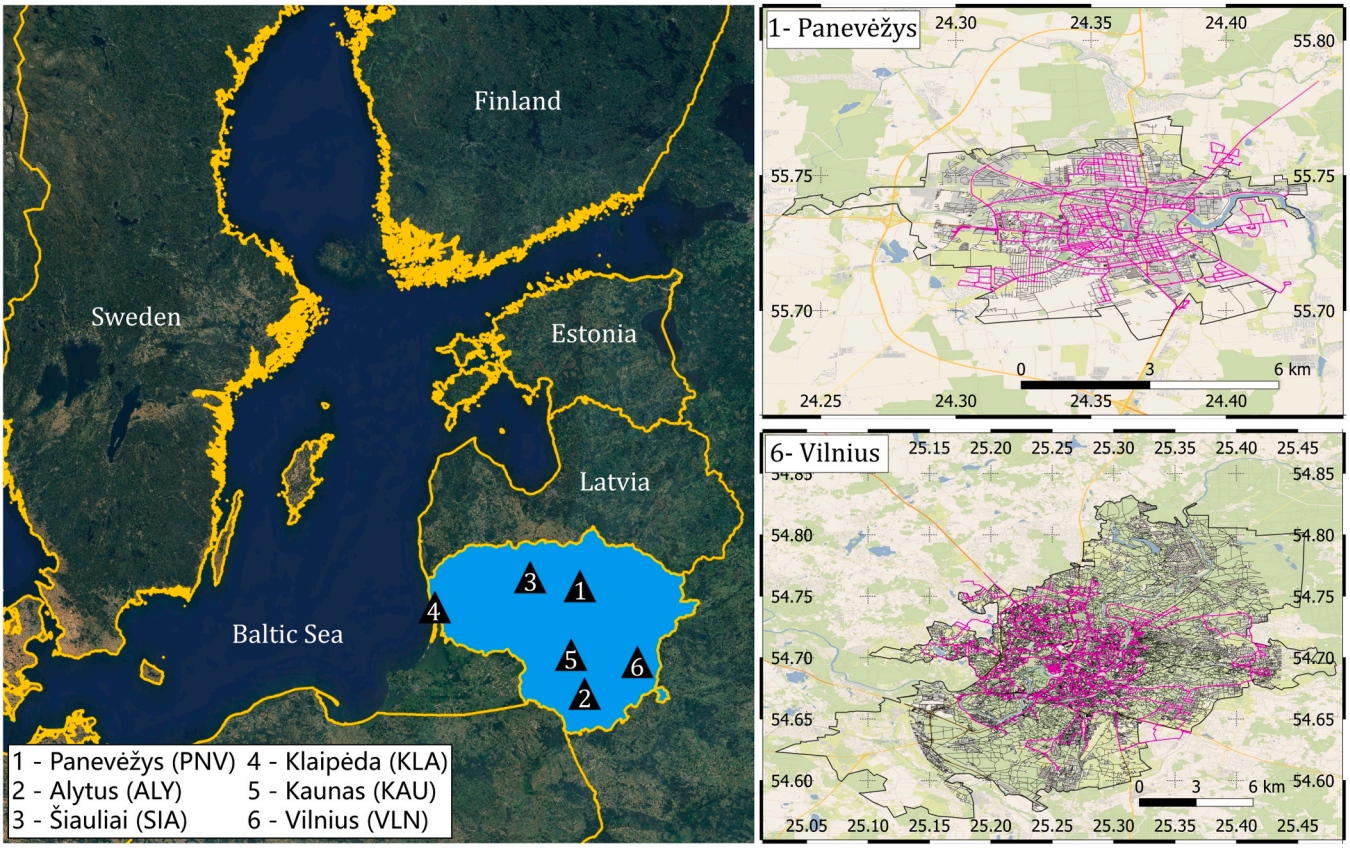

Fig. 2. Measurement domain in Northern Europe, Lithuania. The numbers indicate measurement sequence in six Lithuania cities. On the right – an example of city specific spatial extent of the measurements. Other city maps are available in supplementary information (SI, Fig. S1-S6).

Table 1
Summary of mobile pollution measurement (during the days indicated in column Date) in Lithuania. The meteorological information (wind speed (WS), wind direction (WD), temperature (T), pressure (P), and relative humidity (RH)) is taken from official measurement sites operated by Lithuanian Hydrometeorological Service [38]. Population data is obtained from State Enterprise Centre of Registers [66]. Other parameters include the average (± standard deviation) driving speed given as V; total driven distance (S) and driven distance per day (± standard deviation); # - total measurement points.

Date	City	Population	Area, km^2	WS, m/s	WD, deg	T, C	P, hPa	RH, %	V, km/h	S, km (S/day)	#
2024–06–20 2024–06–21 2024–06–25 2024–06–26	PNV	88363	51.8	2.3 ± 2.5	302 ± 55.0	22.4 ± 3.5	1017.0 ± 2.1	49.1 ± 13.6	25 ± 12	514 (129 ± 9.3)	76453
2024–07–08 2024–07–09 2024–07–10 2024–07–11	ALY	52034	64.7	1.8 ± 2.8	102±48.0	25.9 ± 3.9	1020.0±3.0	47.3 ± 21.3	24 ± 10	526 (131 ± 7.9)	88880
2024–07–15 2024–07–16 2024–07–17 2024–07–18	SIA	121288	166.8	1.1 ± 2.2	217 ± 66.3	24.2 ± 3.6	1016.0 ± 2.0	51.5 ± 11.7	23 ± 10	530 (133 ± 31.1)	105078
2024–07–22 2024–07–23 2024–07–24 2024–07–25 2024–07–26	KLA	170519	221.2	1.8 ± 1.5	293 ± 59.0	21.0 ± 2.1	1013.0 ± 1.3	71.8 ± 9.7	22 ± 11	653 (131 ± 17.5)	130501
2024–07–30 2024–07–31 2024–08–01 2024–08–02	KAU	314208	222	3.3 ± 1.8	308 ± 49.3	21.2 ± 2.0	1010.0 ± 2.0	56.2 ± 8.7	27 ± 12	790 (198 ± 25.6)	139718
2024–08–06 2024–08–07 2024–08–08 2024–08–09	VLN	632476	314.6	0.9 ± 1.8	314.±37.5	21.9 ± 2.5	1013.0 ± 1.0	65.0 ± 15.3	25 ± 12	689 (172 ± 28.9)	137935

Lithuania: Vilnius (VLN), Kaunas (KAU), Klaipėda (KLA), Šiauliai (SIA), Panevėžys (PNV), and Alytus (ALY). The total population in the six measurement cities comprises nearly half (48 %) of the country's population. These cities were therefore selected to represent a significant and diverse portion of the national urban landscape in terms of both population density and traffic activity. The measurement domain covers a wide range of roads and traffic scenarios. Collectively, the measurements covered a cumulative area of 1000 km^2 and took 25 days to complete. In all cities, except Vilnius, the predetermined measurement route covering the whole city area was traversed in a single day. For PNV, ALY, SIA, KLA, and KAU, the spatial measurement data consequently represent an average value recorded from repeat traverses over four to five days. Meanwhile, as Vilnius city area is 1.4–6.0 times larger than the other cities, it was not possible to cover the entire city area in one day. In this case, the routes were split into two and were driven twice over four days. Vilnius, the capital of Lithuania, has the highest population and the largest number of registered light-duty vehicles (M1, vehicles with fewer than eight seats), reaching approximately 325000 vehicles [57]. Notably, Vilnius has the lowest proportion of diesel-powered vehicles (50 %), whereas all other cities exceed 60 %, with Panevėžys leading at 70 %. This diverse urban and vehicular landscape offers a unique opportunity to analyze varying road-traffic characteristics and their impact on emissions and air quality. The mean temperature during the campaign ranged between 21 and 26 °C. Although the measurement platform (Fig. 2) was designed to withstand substantial rain, the measurements were performed during non-raining days to maintain measurement consistency. On average, the workday measurements started at 10 AM and finished between 5 and 6 PM local time.

3.2. Experimental set-up for mobile pollution measurements

3.2.1. Mobile measurement trailer

A specialized mobile measurement trailer was developed for this study as depicted in Fig. 3. A single axle trailer (1300 kg; with a rear ramp, front window, and side doors) with inner dimensions of 3.0 × 2.0 × 2.1 m (height x width x length, respectively) was installed with instrument racks, using rubber supports to dampen the vibrations and a water-proofed aerosol sampling inlet. The aerosol inlet tube (inner diameter 14 mm) extended 1.5 m above the roof and was equipped with a PM_{10} inlet (the cut-off diameter of 10 μm). Inside the container, the aerosol was directed to a diffusion dryer (0.5 m long; with approx. 2 kg of silica gel beads), specifically designed for this study [30]. The aerosol was split after the diffusion dryer into two flows (6.6 and 10 l/min) using a custom made isokinetic flow splitter. The splitter and instruments were connected with 0.7 m of conductive tubing. The total sampling flow of an aerosol was chosen to be 16.6 l/min (complying with the PM_{10} inlet), which resulted in an overall aerosol residence time in the sampling line of approx. 1.5 s. The supplementary equipment included a high-volume oil and regular membrane vacuum pumps (for aerosol sampling), a compressor (for silica gel drying, when not measuring) with a dehumidifier and particulate filter, as well as an air conditioning unit connected to the outside through a vent ensuring clean air circulation inside the measurement container. The vacuum pump outlet was directed to an outside vent to prevent oil droplet laden air accumulation inside the cabin. The electrical power was provided through a pure sine wave inverter (PSW 2002 W - 12 V, Gys, France), which was used to convert power from 12 to 220 volts. Throughout the mobile measurement campaign, the specialized measurement trailer was towed by a diesel-powered vehicle, with precautions taken to ensure that exhaust emissions from the towing vehicle did not influence the measurements (Fig. 3).

3.2.2. Particle measurements

The PNSD (normalized by logarithmic channel width, $dN/d\log d_p$; N being particle number concentration in $1/cm^3$; d_p – particle size in nm) were measured using a high-resolution electrical low-pressure impactor (HR-ELPI, Dekati, Finland), which combines impaction and electrical detection to classify particles based on their aerodynamic diameter [29]. The HR-ELPI measures particles in 14 size fractions in the range from 6 nm to 10 μm. The instrument was successfully applied in both field and laboratory studies utilizing its high temporal resolution (e.g., [53, 10,39]). During the measurement campaign, sintered metal impaction plates were used to minimize impactor overloading and particle bounce. The instrument uses an aerosol flow of 10 l/min provided by a vacuum pump operating at 420 l/min at 40 mbar. The PNSDs were recorded at 1 Hz time resolution through a dedicated Dekati software, which besides data acquisition, also allows instrument control and status monitoring. Instrument operation and maintenance procedures were strictly followed as described in the instrument user's guide and included periodic (after measurement cycle in one city) disassembly of the impactor stages and cleaning it in an ultrasonic isopropanol bath for several hours. Impactor leakage test, as well as electrometer zeroing (for 30 min) were performed before each measurement day or instrument turn on. Internal instrument calibration curves, correction, dilution value and other parameters required to run the instrument were adopted from the user manuals and recommendations by the instrument manufacturer.

The eBC (obtained by converting measured optical attenuation into a mass concentration using an assumed mass-absorption cross-section) was measured using micro aethalometer (MA200, AethLabs, USA). The instrument measures optical attenuation from aerosol laden filter across five optical wavelengths: 880, 625, 528, 470, and 375 nm. In this work, eBC is assessed via the 880 nm channel. The instrument was set to one second time resolution, with a flowrate of 100 ml/min. Before each measurement cycle, instrument was let to stabilize for 30 min (in parallel with HR-ELPI electrometer calibration/zeroing).

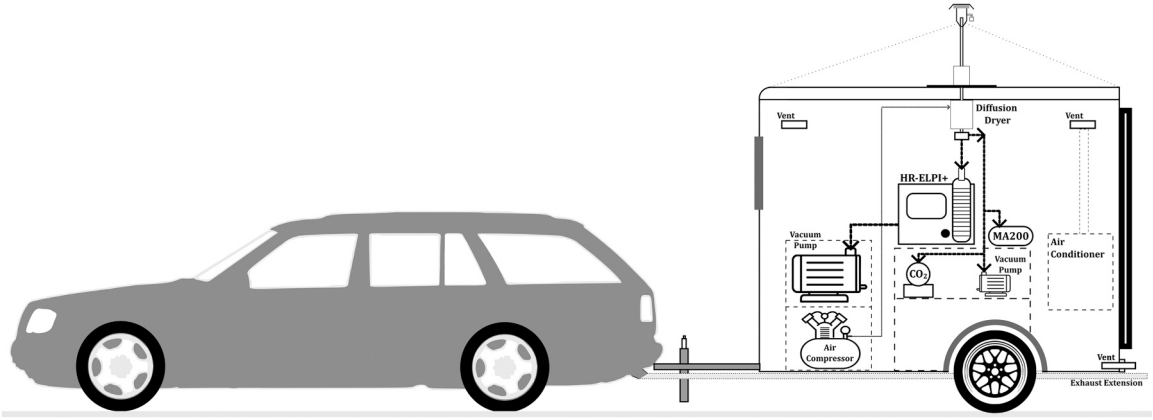

Fig. 3. A simplified sketch (not to scale) of the measurement trailer developed for the study.

Supplementary information, such as carbon dioxide (AX-5000, China), aerosol sample temperature and relative humidity (RH; HYT939, IST AG, Switzerland), as well as street videos (not discussed in this work) were recorded with a combination of low-cost sensors and a single-board computer (Raspberry Pi, UK).

3.3. Particle data processing

3.3.1. High-resolution particle number size distribution

The recorded raw PNSD data in 14 bins were recalculated to high-resolution data (500 bins) representation using proprietary Data Analysis Tool software, provided by Dekati (Finland). After consultation with the instrument manufacturer, the density parameter was set to 0.8 to adjust PNSDs to presence of black carbon aerosol. The size selective particle losses in the plumbing lines were evaluated using the formalism presented by von der Weiden et al. [73]. Further data processing included removal of calibration and zero measurement periods, and instances when impactor pressure reading was out of the 40 ± 5 mbar range. The resulting total number of 1 s measurement instances per city is given in Table 1. From measured PNSD, particle number concentrations were categorized (by integrating normalized PNC in appropriate size ranges) into ultrafine (UFP; particle diameter (d_p) < 100 nm), accumulation (ACCU; 100 ≤ d_p < 1000 nm), coarse (COARSE; 1 ≤ d_p ≤ 10 μm) modes and total particle concentration (d_p from 6 nm to 10 μm). The same size ranges were used to represent size-resolved particle surface area concentration following Eq. 1:

$$S = \int_{d_{min}}^{d_{max}} \pi d_p^2 \frac{dN}{dlog(d_p)} dlog(d_p) \quad (1)$$

where, S is the (spherical-) equivalent surface area concentration (in $\mu m^3/cm^3$), d_{min} and d_{max} - minimum and maximum particle diameters in the size distribution, d_p – particle diameter, and $dN/d\log(d_p)$ - number concentration per logarithmic bin width. The integration in Eq. 1 is performed by summation over all 500 size bins. Furthermore, Eq. 1 assumes that ambient particles are spherical, which may not accurately represent the morphology of urban aerosols. Therefore, it is important to note that Eq. 1 yields an "equivalent" particle surface area. For simplicity, this is referred to as "particle surface area" throughout this work.

3.3.2. Equivalent black carbon

The raw eBC measurements from the aethalometers, especially those recording at the highest time resolution of one second, were often distorted by the occurrence of negative values in eBC data sets [21,41]. This was because of the presence of instrumental optical and electronic noise, associated with the high sample rate (1 Hz), which leads to periods with cumulative light attenuation values remaining static or even decreasing over the 1 s sampling time per data point. For this reason, the raw eBC measurements were treated using the optimized noise-reduction averaging algorithm (ONA) proposed by [21]. The threshold value for the attenuation difference was empirically set to 0.001, which reduced negative values to nearly zero, retaining high resolution concentration variability. Last but not least, only the measurement values associated with driving speed (v_d) above 5 km/h were used in data analysis to avoid pollution from the trailer towing vehicle.

3.3.3. Lung deposited surface area concentrations

In this work, we used the metrics of respiratory tract deposited particle surface area concentration and deposited surface area dose. Pulmonary particle dose is more predictive of toxicological effects than particle concentration, since lung-deposited particles only – not mere inhaled particles – can induce toxicological effects [62]. Assessing respiratory deposition dose rather than merely ambient exposure concentration provides a more accurate metric of the actual burden of inhaled particles on the human respiratory tract, as it accounts for factors such as particle size–dependent deposition efficiency and individual breathing patterns and time-activity profile [22]. Analogous to exposure concentration, pulmonary deposition dose can be expressed in mass, number, or surface area per minute metrics, each of which correlates differently with adverse health outcomes, with surface area often being the most relevant for nanoparticle toxicity due to its relationship with cellular interaction sites [33,36] even for soot particles with different primary diameter and organic carbon content [69]. By contrast, ambient concentration measurements ignore the variable fraction of particles that deposit in bronchial, tracheobronchial, and alveolar regions, potentially underestimating or overestimating dose depending on individual ventilation rates and time-activity record [22]. Incorporating deposition dose thus enables more precise health risk assessments and exposure–response modeling in environmental studies, as it reflects the biologically effective dose delivered to lung tissues [44]. Moreover, deposited surface area concentration has been shown to better predict pulmonary inflammation and oxidative stress than mass concentration, particularly for ultrafine particles, underscoring its importance in epidemiological and toxicological investigations [33,36].

Although the HR-ELPI provides internally calculated LDSA concentration, we have chosen to re-calculate LDSA based on obtained PNSD and available total-lung and alveolar deposition fraction curves from the literature (Fig. 4). We did this to expand the LDSA metric to alveolar region, as instrument does not provide this information automatically. Yet, the alveolar region is often considered the most vulnerable region of the lung with respect to inhaled particulate matter. It is important to note that the respiratory tract deposition curves presented here are derived under varying conditions—including differences in minute ventilation, levels of physical activity, and the use of laboratory-based studies and models—and should therefore be considered as generalized averages. Nevertheless, the conversion from airborne concentration to inhaled dose can be reasonably approximated using deposition curves corresponding to resting or light physical activity, with adjustments made according to the volume of air inhaled over a given time period [63].

Following the retrieved deposition fraction curves (in a size range from 10 nm to 10 μm) from the literature, total respiratory and alveolar deposited particle number size distributions were calculated as:

$$\frac{dN_{deposited}}{dlog(d_p)} = \frac{dN}{dlog(d_p)} \cdot DF(d_p) \quad (2)$$

where $DF(d_p)$ is the total or alveolar deposition fraction for a given particle size. The total, ultrafine, accumulation, and coarse deposited surface area concentrations were calculated using Eq. 1 by substituting $dN/d\log(d_p)$ with $dN_{deposited}/d\log(d_p)$ from Eq. 2. Finally, size segregated deposited surface area dose in the alveolar region was calculated using:

$$DD = \int_{t_1}^{t_2} \int_{D_{p1}}^{D_{p2}} \pi d_p^2 V_T f \frac{dN_{deposited}}{dlog(d_p)} dlog(d_p) dt, \quad (3)$$

where V_T is tidal volume (L/breath) and f – breathing frequency (breath/min). In our deposited dose calculation, we assumed V_T and f to be 1.5 L and 17 breaths/min, respectively, corresponding to a brisk walking pace (5.1 km/h), a condition similar to "light exercise" as defined by the Intergovernmental Commission for Radiation Protection [68]. Such values were chosen for the simplicity of calculating the inhaled air volume per one breathing cycle and the distance walked (5 m/breath) at the same time representing somewhat real-world scenario of active walking [48]. The commuting routes were synthetically generated, as real mobility data was not available for this study. Start and end points were randomly selected from a predefined network of walkable urban paths, and the shortest routes between them were computed. Following this procedure, 1000 unique routes were produced, which were then limited to a maximum length of 5.1 km to ensure completion within approximately one hour—facilitating consistent dose calculations. Each

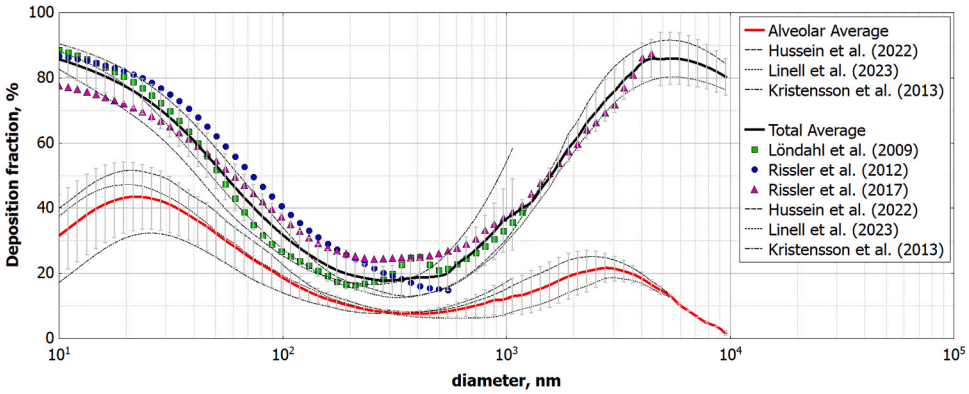

Fig. 4. Size-dependent deposition curves reported in previous studies (experimental and model) and averaged DF for total respiratory and alveolar regions used in this study (solid black and red lines, respectively).

route was discretized at 5 m intervals to represent individual breaths, and LUR-derived pollutant concentrations were assigned at each point for exposure estimation. While this approach does not reflect true commuting behavior, it provides a uniform spatial distribution of routes across the urban area. This contrasts with real-world mobility patterns, which tend to be concentrated along major corridors. However, the randomized method offers the advantage of enabling standardized, city-wide comparisons and ensures representation of diverse urban settings, including high-traffic zones, residential areas, and green spaces. As such, it supports a generalized assessment of exposure variability across the entire urban environment, offering insights into potential inhaled dose distributions even in the absence of personal mobility data.

3.4. Land use regression modeling

Land use regression is a statistical method used to estimate spatial variations in environmental exposures, i.e. air pollution by linking measured pollutant concentrations as model outcomes to geographic predictors like traffic, land use, greening and other geographical features (e.g., [46,60]). We selected LUR modeling rather than dispersion modeling for estimating spatial pollution maps because dispersion approaches demand detailed, site-specific physical parameters—such as vehicle emission factors stratified by fleet composition along with high-resolution meteorological inputs—to accurately simulate pollutant release, transport, and transformation [12,2]. In contrast, LUR models utilize readily available geographic and land-use predictors (e.g., traffic density, road network metrics, population distribution, etc.) to estimate ambient pollutant concentrations without requiring exhaustive emission inventories [15,25]. This methodology therefore minimizes the complexity and uncertainty inherent in parameterizing diverse emission sources and dispersion physics, while still delivering robust spatial resolution and predictive accuracy suitable for epidemiological assessments [3].

For the land use regression modeling, measurement count and median values in 50 × 50 m grid were computed from cleaned measurement data (see Section 3.3). The deposited surface area concentrations were predicted using five different categories of variables. The land use, buildings, and road network information were obtained from the Open Street Map services [50]. Additionally, traffic noise and altitude information was sourced from the European Environment Agency Central Data Repository [16] and the Lithuanian Spatial Information Portal [45]. The area (land use, building coverage), length (roads), average altitude and noise levels were computed within 50, 100, 500, and 1000 m buffers for all grid cells. The selection of these buffer sizes was driven by the need to balance predictive performance and computational efficiency.

Because the created grids did not always align perfectly with roads at different angles, several instances occurred when specific grid cells only had a few measurement points. In such instances, cells with fewer than 4 measurement points were removed from the data set, preserving 93–96 % of the data. Given the non-normal distribution and high skewness of the data, we applied a logarithmic transformation to the pollutant variable and a scaling transformation to feature variables, to improve the model's performance.

An extreme gradient boosting (XGBoost; [9]) regression models were trained to predict alveolar deposited surface area concentration based on measured PNSDs in the six cities in Lithuania and multi-source spatial data. More details about the models is available in the SI. Three different models (per each city) were developed to represent contributions of ultrafine, accumulation, and total particle surface area concentrations deposited in alveolar region of the respiratory tract. Ultrafine and accumulation mode particle models are not shown here (are available upon a reasonable request from the corresponding author). The best-performing model, along with cross-validation and test set R^2 values, best model hyperparameters, and other relevant model information, is presented in Table T1 (SI). The final model was selected based on the best R^2 score on the validation folds and further evaluated on the independent test set. Model performance for predicting total alveolar deposited surface area concentration varied across cities and particle modes, with test set R^2 values ranging from 0.38 to 0.65. The ultrafine mode generally showed moderate predictive power ($R^2 \approx$ 0.38–0.59), while the accumulation mode yielded slightly lower but comparable values ($R^2 \approx$ 0.38–0.61). The total particle models performed best overall, with R^2 values between 0.47 and 0.65, reaching their highest in KLA and KAU. This indicates reasonably good model generalizability, particularly for total surface area predictions. The most important features (top 10) are listed in Table T2 (SI).

3.5. Software

Measurements were evaluated and analyzed using the open-source programming language and software environment R ([56]; version 4.2.2). Open-source tools for air quality data analysis [8] and custom functions were used to investigate eBC and PNSD data. For spatial data statistics, land feature evaluation, and data representation a quantum geographic information system [54] was used. For model training Google Colaboratory (accessed January 2025, Google Research, https://colab.research.google.com/) engined by Python 3.11 (www.python.org) Google Compute Engine backend (GPU with 12.7 GB of System RAM; 15.0 GB GPU RAM; and 78.2 GB of Disk space) was used. Figures were made using R ggplot2 library [75], a cross-platform scientific application for data analysis and visualization ([55]; version 0.9.8.3), and free graphical design tool Inkscape (version 1.2, 2020).

4. Results and discussion

4.1. Equivalent black carbon and size-segregated particle number and surface concentrations

Several different airborne pollutant metrics (eBC mass, size segregated particle number concentrations, as well as different mode number fractions) across six Lithuanian cities reveal distinct spatial trends and source influences (Fig. 5; Table T3). The measured eBC and PNC data showed a strong skewness to high values, that is, during encountering pollution plumes from nearby vehicles, eBC and PNC mass and number concentrations respectively increased by several orders of magnitude. Subsequently, with no vehicles present, the measured pollutant concentrations decreased to urban background values. We extracted the urban background pollutant concentrations (concentration deconvolution) by applying the 25th percentile with a rolling window of 20 min (value determined empirically, based on visual inspection of resulting background concentration variation over all measurement period; e.g., [34,31]).

The analysis of eBC concentrations (Fig. 5; Table T3) revealed notable differences among the six cities. Vilnius recorded the highest mean eBC concentration at 3236 ng/m^3 , driven by its large population and intense traffic activity. In contrast, Šiauliai exhibited the lowest mean concentration at 2092 ng/m^3 . Interestingly, Panevėžys, a smaller city, showed a high mean eBC of 3170 ng/m^3 , largely due to its substantial proportion of diesel vehicles, which accounted for 69.6 % of its fleet. Variability in eBC levels was most notable in Vilnius, where the standard deviation reached 3723 ng/m^3 , reflecting dynamic emission patterns linked to fluctuating traffic. Background eBC levels, separated from direct emissions through deconvolution, peaked in Vilnius at 710 ng/m^3 and were lowest in Šiauliai at 380 ng/m^3 , underscoring the role of local traffic in shaping urban background pollution. Comparatively, median eBC concentrations in Lithuanian cities exceeded those in Northern and Western European cities like Helsinki and Stockholm (540–800 ng/m^3), but fell below levels in high-traffic hubs such as Milan and London (1890–4800 ng/m^3; [61]). Background eBC medians in Lithuania (330–580 ng/m^3) surpassed those in Nordic cities like Stockholm and Helsinki (190–260 ng/m^3), yet remained lower than in Southern European locations such as Granada and Marseille (1180 ng/m^3), aligning more closely with Central European cities like Bern and Zurich [61].

The PNC across cities show patterns similar to eBC, with Vilnius recording the highest mean concentration ($1.52{\cdot}10^4$ particles/cm^3), followed by Panevėžys and Kaunas (Fig. 5; Table T3). The highest deconvoluted (background) PNC was found in Panevėžys with the mean value of 5150 particles/cm^3 , followed by Alytus, and Šiauliai. The UFP concentrations mirror this trend, with Vilnius, Panevėžys, and Kaunas exhibiting the highest levels (up to $1.27{\cdot}10^4$ particles/cm^3). The smaller city Alytus —show notably lower UFP concentrations ($7.95{\cdot}10^3$ particles/cm^3), reflecting its reduced traffic volumes and less intensive urban activities. Despite being a major coastal port city, Klaipėda exhibits lower UFP concentrations than might be expected, likely due to enhanced pollutant dispersion facilitated by coastal meteorological conditions—a factor absent in inland cities like Vilnius and Panevėžys where urban morphology may impede ventilation. The ACCU particles show the highest concentrations in Vilnius and Panevėžys (approx. 2300 particles/cm^3), followed by Kaunas, Klaipėda, and the rest of cities. These patterns generally align with eBC concentrations, confirming that accumulation mode particles are predominantly associated with combustion processes, particularly diesel engine emissions [31]. The coarse mode particle concentrations exhibit a starkly different pattern, with Klaipėda showing an exceptionally higher concentration (30.0 particles/cm^3) compared to other cities. Kaunas also demonstrates elevated coarse particle levels (20.0 particles/cm^3), while the remaining cities show substantially lower concentrations (1.7–3.2 particles/cm^3). Klaipėda's high coarse particle concentration can be attributed to its coastal location, where sea spray aerosols may contribute to elevated coarse particle loading (e.g., [1,18,13]). Additionally, its function as a port city entails substantial mechanical processes, including dust generation from loading and unloading activities and heavy-duty vehicle movements, further elevating coarse particle concentrations [26,58]. High coarse mode particle concentration in Kaunas can be associated with resuspended dust from several major construction sites across the city. Elevated concentrations of coarse-mode particles in Klaipėda and Kaunas led to increased total particle surface area concentrations (Fig. S7), as well as higher respiratory tract–deposited surface area concentrations and corresponding surface area doses. These effects are further examined in Sections 4.2 and 4.3.

In a European context (e.g. [59]), the median PNC in six Lithuanian cities ranged from 5900 in Šiauliai to 8600 particles/cm^3 in Panevėžys, which is lower than the traffic-influenced median summer PNC observed in some European cities, specifically 8700 particles/cm^3 in Dresden and

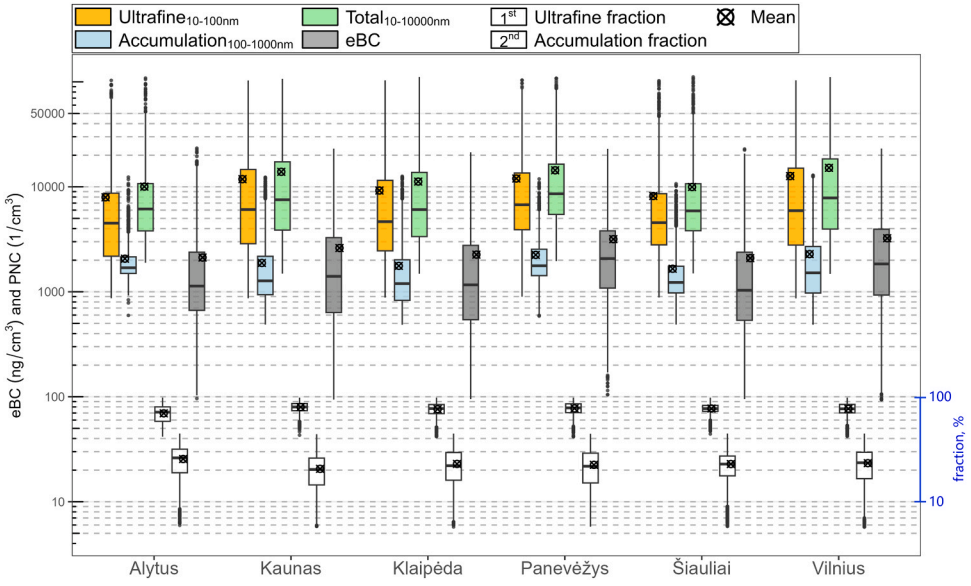

Fig. 5. The measured eBC and size segregated PNC in six Lithuanian cities. White bars represent ultrafine (first of two) and accumulation (second of two) mode number fractions (percentage of total number concentration).

9800–10600 particles/cm^3 in Leipzig, Germany. For background sites, the median PNC in Lithuanian cities (obtained from deconvolution of PNC) varied between 3000 in Klaipėda and 4900 particles/cm^3 in Panevėžys, compared to 4800 in Leipzig and 6900 particles/cm^3 in Prague. Thus, while the street median PNC in Lithuanian cities was consistently lower than in other European cities, the background PNC in Lithuanian cities spanned a range that included values similar to Leipzig but lower than Prague, Czech. Please note that our pollutant statistics were derived from short-term, intensive roadside measurements, whereas the comparison values originate from stationary, long-term monitoring stations. The inherent limitations of these differing methodologies are discussed in detail in Section 4.4.

Particle number fractions reveal the dominance of ultrafine particles across all cities, with ultrafine number fractions ranging from 70 % in Alytus to 80 % in Kaunas. This predominance of ultrafine particles by number is characteristic of fresh vehicular emissions, especially from diesel engines [31]. The higher ultrafine fraction in Kaunas (80 %) despite its lower overall diesel vehicle percentage (60 %) compared to Panevėžys (70 %) suggests additional factors affecting particle size distributions, potentially including more congested traffic conditions leading to more frequent acceleration/deceleration cycles and consequently more ultrafine particle emissions. In contrast to number fractions, surface area fractions reveal the dominance of accumulation mode particles in terms of surface area. Accumulation mode surface area fractions range from 28 % in Klaipėda to 74 % in Alytus. This inversion between number and surface area dominance reflects fundamental aerosol physics—while ultrafine particles dominate numerically, their small size means they contribute proportionally less to overall particle surface area. Notably, Klaipėda exhibits the lowest accumulation mode surface area fraction (28 %) and the lowest ultrafine surface area fraction (7 %), indicating that coarse particles contribute substantially to the total surface area in this coastal city.

4.2. Respiratory tract deposited surface area concentrations

Examining the respiratory tract deposited surface area concentrations, Klaipėda stands out with the highest mean of total respiratory deposited surface area concentration (TDSA, Fig. 6; Table T3) at 570 μm^2/cm^3 , making it roughly three to four times higher than Šiauliai and Alytus, which records the lowest mean TDSA at approx. 130 μm^2/cm^3 , respectively. As already discussed previously, this substantial difference stems from Klaipėda's function as Lithuania's primary seaport, where maritime activities re-suspended dust and sea-spray contribute significantly to accumulation and coarse particle emissions. Despite having fewer light-duty vehicles (77000) than Vilnius (325000), Klaipėda's as a port city emissions appear to overwhelm the contribution from passenger vehicles (emissions of fine particles).

Coarse particles dominate the TDSA in larger cities, with Klaipėda showing 490 μm^2/cm^3 (86 % of TDSA) and Kaunas 270 μm^2/cm^3 (78 % of TDSA). Smaller cities demonstrate a more balanced distribution, with Alytus' coarse particles accounting for 41 % of TDSA, Panevėžys' for 49 %, and Šiauliai's for 47 %. In Kaunas, coarse particle burden can be associated mostly with resuspended dust. The fraction of UFP in TDSA shows a more nuanced relationship with city size. Šiauliai, Panevėžys, and Vilnius exhibit similar percentages, with values around 20 %, suggesting that ultrafine particles from vehicular emissions represent a consistent contribution to total respiratory deposition across these different urban environments. This is particularly relevant in smaller cities like Šiauliai and Panevėžys, where older vehicle fleets and a high percentage of diesel engines (Šiauliai: 63 % diesel, Panevėžys: 70 % diesel) likely contribute significantly to this fraction. By contrast, in Klaipėda and Kaunas, the ultrafine contribution is suppressed by the substantial presence of coarse particles from non-combustion sources, such as port activities, sea-spray aerosol, and resuspended dust.

The analysis of alveolar region deposited surface area concentration (ADSA, Fig. 7; Table T3) followed similar trend to TDSA, with Klaipėda exhibiting the highest ADSA values at 160 μm^2/cm^3 , followed by Kaunas at 100 μm^2/cm^3 . The ranking remains consistent between total and alveolar deposition, suggesting that the mechanisms driving overall deposition also influence deep lung doses. Size segregated analysis of deposited surface area concentration revealed that ultrafine particle ADSA is highest in Vilnius (mean: 20 μm^2/cm^3), likely due to its high traffic volume and dense street network. Accumulation mode ADSA is highest in Vilnius and Panevėžys (approx. 30 μm^2/cm^3). Coarse particles ADSA show extreme values in Klaipėda (120 μm^2/cm^3) and Kaunas (60 μm^2/cm^3), over 15 times higher than in Alytus. When examining ADSA fractions, ultrafine particles constitute higher portions of alveolar deposition than of total respiratory deposition across all cities. Šiauliai,

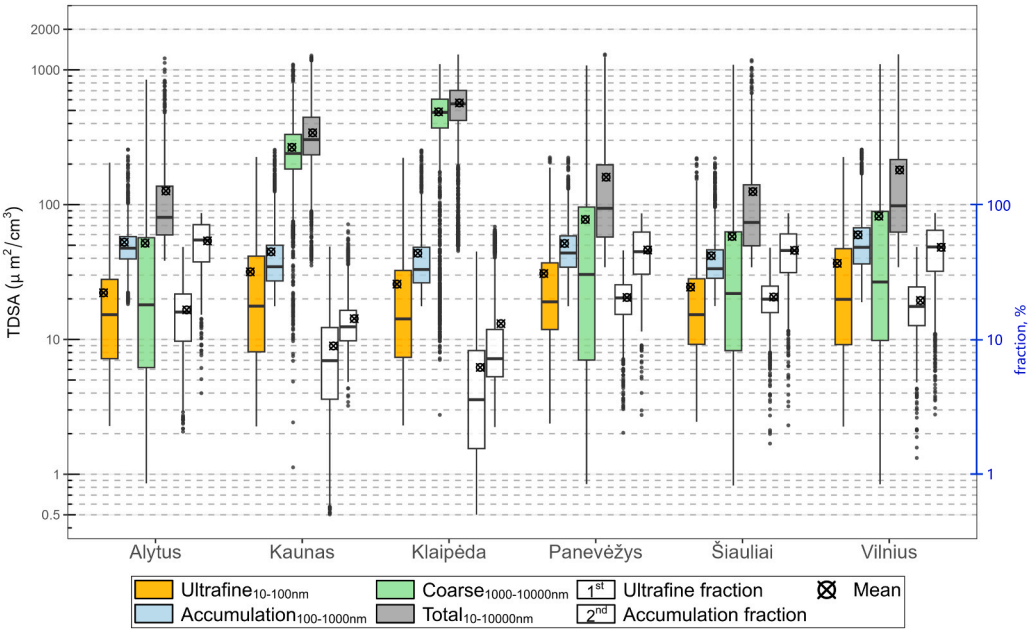

Fig. 6. The calculated total respiratory deposited surface area concentration segregated by different modes (ultrafine, accumulation, and coarse). White bars represent ultrafine (first of two) and accumulation (second of two) mode surface area fractions (percentage of total concentration).

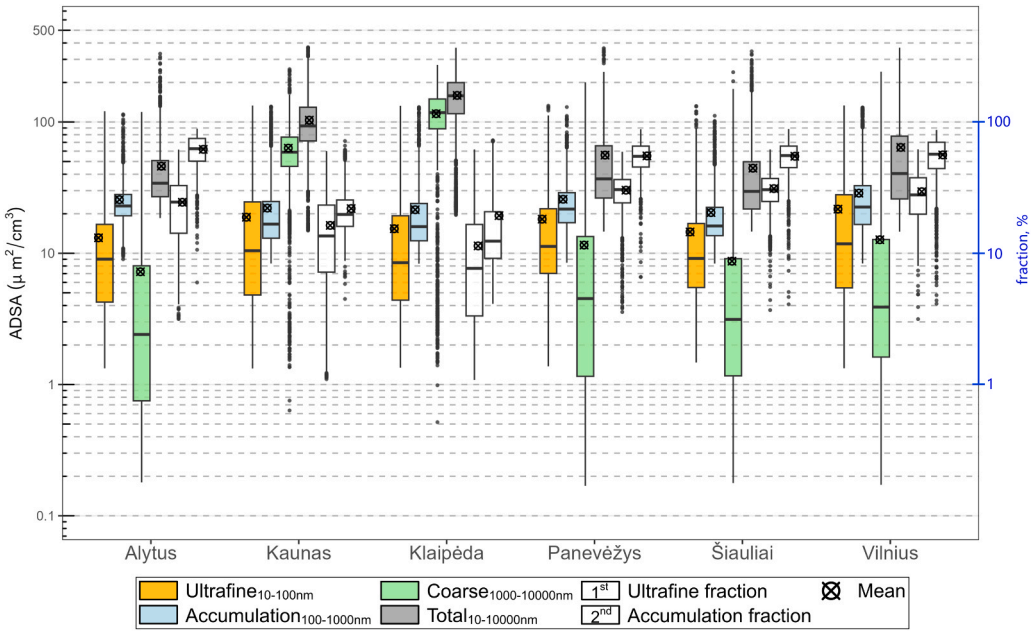

Fig. 7. The calculated alveolar region deposited surface area concentration segregated by different modes (ultrafine, accumulation, and coarse). White bars represent ultrafine (first of two) and accumulation (second of two) mode surface area fractions (percentage of total concentration).

Panevėžys, and Vilnius show the highest alveolar ultrafine fraction (30 %), while Klaipėda shows the lowest (10 %). The ACCU particles dominate alveolar deposition across all cities, accounting for 50–60 % of alveolar deposits.

Street-level median values of UFP + ACCU mode particle TDSA range from 50 to 70 $\mu m^2/cm^3$. These values align with or exceed median LDSA concentrations reported in European cities [42] such as Dresden, Helsinki, Leipzig, London, and Stockholm (30–70 $\mu m^2/cm^3$). For instance, Vilnius (70 $\mu m^2/cm^3$) approaches the upper range observed in Leipzig and London, while Alytus and Panevėžys (both 60 $\mu m^2/cm^3$) slightly surpass Dresden's median values. Nevertheless, the observed TDSA values (from ultrafine and accumulation modes) indicate that inhabitants in Lithuanian urban areas exhibit comparable respiratory deposited surface area concentrations to those in many European urban centers. With that said, in this study, the street-level measurements include additional coarse mode particles (which are not accounted in a study by [42]), leading to significantly higher total LDSA concentrations. Accounting for coarse particles, median TDSA values in Lithuanian cities far exceed European LDSA values (which exclude coarse particle mode). For example, Klaipėda's median TDSA (including coarse mode) is approximately 8–18 times higher than median European street LDSA values (30–70 $\mu m^2/cm^3$), underscoring the significant contribution of this mode to TDSA in Lithuania. Background TDSA concentrations (obtained using measured data and deconvolution algorithm) follow a similar pattern. Median TDSA (accounting for ultrafine and accumulation mode particles) levels in Lithuanian cities range from 30 $\mu m^2/cm^3$ (Klaipėda) to 50 $\mu m^2/cm^3$ (Alytus), comparable to European background LDSA medians [42] such as Athens, Dresden, and Madrid (40–50 $\mu m^2/cm^3$). However, non-combustion related appearance of coarse particles elevates TDSA concentrations in Lithuania, particularly in Kaunas (median = 250 $\mu m^2/cm^3$) and Klaipėda (490 $\mu m^2/cm^3$). These values starkly contrast with European background data, which often lacks coarse mode measurements.

4.3. Deposited alveolar particle surface area dose based on population commuting proxy

In this study, we assess lung-deposited surface area concentration and corresponding doses for pedestrians in diverse urban environments—ranging from traffic corridors to tranquil parks—by integrating extensive mobile monitoring and high-resolution LUR modeling. This dual approach allows us to quantify respiratory deposition doses when commuters are directly exposed to traffic emissions versus when they traverse routes buffered by vegetation or residential zoning. The example of Panevėžys is presented in Fig. 8, where the pollution map of alveolar deposited surface area concentration is presented including randomized routes for calculating the deposited dose per 1 km commuted. The other corresponding for the other cities is provided in SI (Fig. S8-S13). The alveolar deposited dose (ADD) statistics for all cities is presented as box plot in Fig. 9 and Table T3. Kaunas records the highest ADD at 40 mm^2/km, followed by Klaipėda (30 mm^2/km). Vilnius and smaller cities such as Panevėžys, Šiauliai, and Alytus show lower values. Examining mode-specific ADD, the deposited dose of ultrafine particles ranged from 6 (Alytus) to 8 mm^2/km (Kaunas). The accumulation mode dose although highest in Vilnius (12 mm^2/km), were closely matched by values in Panevėžys, Kaunas, and Klaipėda (11 mm^2/km). Coarse mode particle ADD was particularly pronounced in Kaunas (19 mm^2/km) and Klaipėda (14 mm^2/km), consistent with observed highest respiratory deposited surface area concentration values.

The highest ADD ultrafine fraction was found in Panevėžys and Šiauliai (approx. 30 %), which aligns with older vehicle fleets and high diesel shares (70 % and 60 %, respectively), emitting higher levels of ultrafine particles. This showcases the importance of ultrafine particles for respiratory deposition (and thus possible negative health-related outcomes) in cities where diesel vehicles dominate emissions. Vilnius also exhibits a high ultrafine fraction (30 %), most likely due to its heavier traffic congestion (stop-start moving traffic). In contrast, Kaunas and Klaipėda showed the lowest ultrafine particle deposition fractions (approx. 20 %), because these cities have substantial contributions from larger, coarse particles that dominate overall deposition. The accumulation mode particle dose fraction is most pronounced in Alytus, Vilnius, and Šiauliai (40–50 %). In Kaunas and Klaipėda, the accumulation fraction is lower - approx. 30 %. Future health risk assessments shall move beyond conventional ambient concentration metrics and incorporate alveolar deposition dose metric, which quantifies the number/surface area/mass of inhaled particles deposited in the deepest regions of the lung. Incorporating ADD into risk frameworks enables a direct

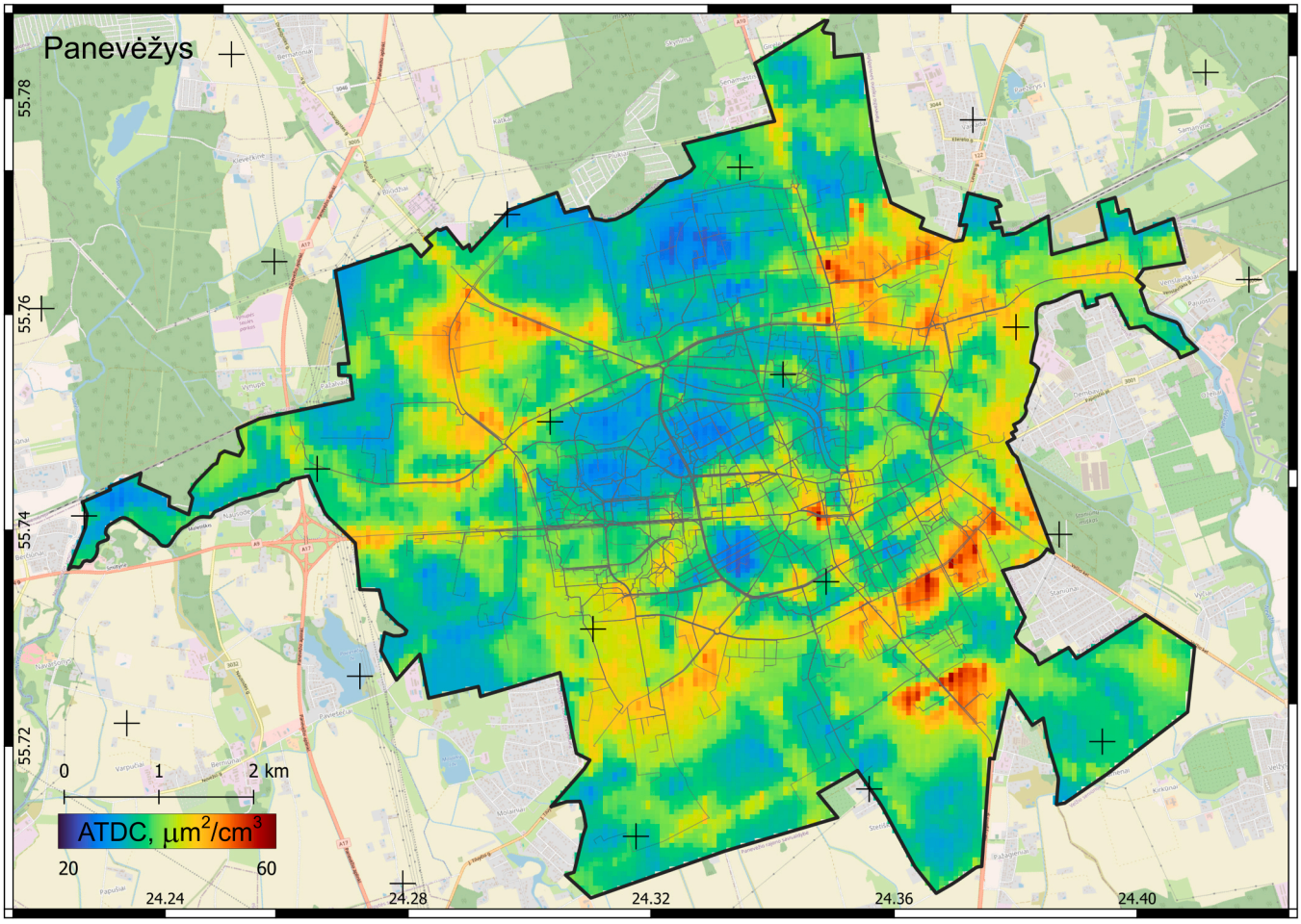

Fig. 8. Exemplary case of total alveolar deposited surface area concentration with overlaid roads for assessing the population proxy deposition dose while randomly walking in the city.

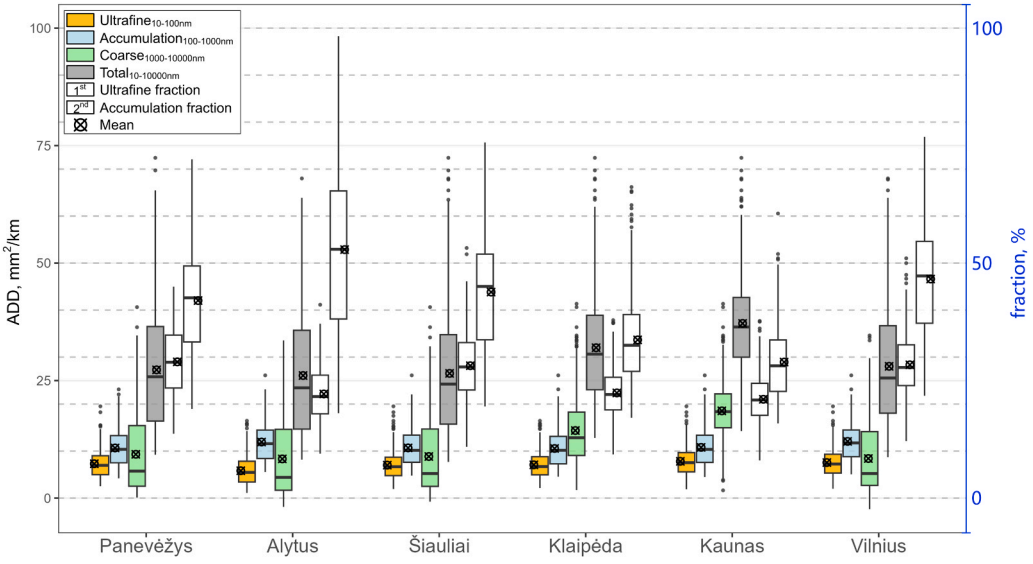

Fig. 9. City-segregated statistics of alveolar deposited surface area dose per 1 km commuting.

mechanistic link between external exposure and internal dose, thereby improving the reliability of dose–response relationships. This approach also allows to account for inter-individual variation in commuting and breathing patterns, airway morphology, and clearance kinetics, all of which modulate actual deposition.

4.4. Limitations and future research outlooks

4.4.1. Particle deposition dose assessment

The estimation of particle deposition doses in our study depends critically on two parameters: minute ventilation and deposition fraction, both of which carry inherent uncertainties that must be carefully acknowledged. Minute ventilation values were adopted from literature reporting average conditions—typically adults engaged in light urban commuting. These proxy estimates do not account for individual differences in age, sex, fitness, or precise activity level, and thus may systematically under- or over-estimate respiratory intake for atypical subgroups (e.g. older adults, highly fit individuals, or sedentary commuters). For example, Bennett et al. [4] observed that females inhaled slightly higher fractional deposition than males, even though males had substantially higher minute ventilation, leading to a 30 % higher deposition rate overall.

The deposition fractions, while robust and well-validated, were derived from a limited selection of studies using specific subject groups and particle types, which restricts their generalizability. They do not fully represent the diversity of real-world aerosol types—such as organic aerosols, metallic particles, fibers, or hygroscopic materials—or the full population spectrum. For instance, modeling work has shown that children (especially around age 5) may have ~10–20 % higher DF for ultrafine particles in the alveolar region compared to adults, due both to anatomical differences and higher weight-normalized minute ventilation [40]. Moreover, physiological factors—such as lung geometry, airway resistance, and breathing mode (nasal vs. oral)—varied across age and health status, yet are often simplified in standard models. While our estimates rely on the most comprehensive data available, these uncertainties imply the dose estimates may lack precision for certain subpopulations—especially young children, the elderly, or individuals with respiratory conditions. Nevertheless, we have mitigated some of these limitations by using review-based literature for ventilation and deposition parameters and cross-validating our results against published urban commuting exposure studies. Together, these strategies support the reliability of our dose assessment within the known bounds of uncertainty.

Future research could enhance the accuracy of respiratory deposition dose assessments by developing population-specific models for breathing rates and deposition curves, tailored to diverse demographic and physiological profiles. Integrating cohort-based spirometry results into exposure studies would provide detailed, individualized data on respiratory parameters, such as tidal volume and breathing frequency, which vary significantly across age, sex, fitness levels, and health conditions. Furthermore, establishing respiratory deposition curve measurements as a standard medical procedure alongside routine cohort assessments, such as blood panels or cardiovascular screenings, could standardize the collection of particle deposition data in clinical settings. This approach would enable more precise estimation of particle deposition in the respiratory system by capturing inter-individual variability and particle-specific interactions, such as those for ultrafine, black carbon, or organic aerosols. By combining these measurements with longitudinal cohort studies, researchers could develop comprehensive deposition models that reflect real-world variability, ultimately improving the precision of health risk assessments for air pollution exposure across diverse populations.

4.4.2. Temporal and spatial sampling limitations

Short, non-concurrent measurement intervals can introduce significant bias when attempting to compare pollution levels across multiple cities. Episodic meteorological phenomena—such as temperature inversions that trap pollutants near the surface or bursts of regional turbulence that disperse them—occur on timescales shorter than typical monitoring campaigns and can lead to anomalous peaks or troughs in recorded concentrations [37]. Moreover, sampling cities sequentially rather than in parallel fails to account for synchronized human behaviors—such as national holiday travel or variations in heating demand—that modulate emissions. Additionally, the chosen measurement window, typically from 10 AM to 5–6 PM, meant that highly dynamic periods such as the morning rush hour were not fully captured. This strategic choice, while optimizing for consistent daytime conditions, implies that our findings might not fully represent the peak exposure levels occurring during these specific, often more polluted, periods. As a result, observed differences among cities may reflect the timing of the campaign rather than intrinsic urban characteristics. Statistically, short windows reduce the ability to capture low-frequency events and undermine confidence when extrapolating to annual or multiannual averages [37]. This study focuses on summertime urban aerosols primarily sourced from road traffic, excluding influences from winter heating or long-range transport of biomass burning products. As indicated in Table 1, meteorological conditions remained relatively consistent throughout the measurement campaign, suggesting that the observed results are predominantly driven by traffic patterns, the urban road network, and building configurations rather than meteorological variability.

Extending the presented methodology to diverse geographical and socio-economic contexts would enhance its global applicability. While this study focused on Lithuanian cities, applying our approach to megacities, rural areas, or regions with different vehicular fleets and emission profiles (e.g., Asia or Africa) could reveal unique exposure patterns and inform context-specific interventions. International collaborations could standardize respiratory tract deposition modeling, facilitating cross-country comparisons and contributing to global air quality frameworks.

4.4.3. Hygroscopicity and deposition modeling

Aerosol hygroscopicity—defined by the particle's propensity to absorb water vapor at depending on relative humidity—dramatically alters size, density, and aerodynamic behavior as particles traverse the respiratory tract. Under high humidity conditions, as encountered in the lung (close to 100 %), hygroscopic growth can increase particle diameters by tens of percent, shifting deposition from larger airways to deeper lung regions [47]. Empirical studies demonstrate that accounting for hygroscopic growth yields closer agreement with measured deposition fractions, whereas its omission can lead to substantial errors in dose estimation [11]. In this study, it is anticipated that the measured urban aerosols will primarily comprise primary emissions from tailpipes, resuspended road dust, non-exhaust sources, and aged urban aerosols. In the specific case of Klaipėda, the aerosol composition may also include fresh and aged sea-salt particles. Previous research, such as Koehler et al. [35], Vu et al. [74], and Diapouli et al. [14], indicates that hygroscopic particle growth is negligible for fresh emissions and non-road emissions, including resuspended dust. It is thus expected that errors resulting from not accounting for particle hygroscopicity in these measurements will be minimal. Nevertheless, future studies may benefit from incorporating the hygroscopicity parameter when evaluating the health effects of urban aerosols within a respiratory deposition framework. Moreover, expanding mobile measurement campaigns to incorporate real-time chemical speciation of particulate matter, such as through aerosol mass spectrometry or advanced spectrometry techniques, would enable a more granular understanding of source-specific contributions to the respiratory tract deposited dose. For instance, distinguishing between combustion-related (e.g., diesel emissions) and non-combustion-related (e.g., resuspended dust, sea-spray) sources could refine exposure assessments and inform targeted mitigation strategies. Such advancements would be particularly valuable in urban environments like Klaipėda, where maritime activities contribute significantly to coarse particle emissions, as observed in our study.

Technological innovation presents another promising avenue for extending this work. Developing low-cost (below $500), portable sensors capable of measuring ultrafine particle and/or black carbon number concentration/size distribution in real-time would democratize air

quality monitoring, enabling community-driven initiatives and citizen science projects. Such sensors could complement existing monitoring networks, providing high-resolution data for local decision-making and public awareness campaigns.

4.4.4. Health metric selection and necessity of chemical speciation

Although deposited surface-area concentration may serve as a useful proxy for insoluble particles, for soluble aerosols, particularly sea-salt particles prevalent at coastal sites (e.g. in Klaipėda), our study may overemphasize the burden of health-related high-surface-area, since inhaled sea-salt is non-toxic. Without detailed chemical composition data, we are not able to attribute observed particle loads to resuspended dust or aged sea-salt aerosol. In its absence, the assessment remains grounded in physical dose metrics alone, potentially obscuring critical links between emission sources and health outcomes. Unfortunately, no mobile instruments are currently available that can provide online measurements of hygroscopicity or chemical composition with a temporal resolution on the order of seconds.

Also, particle shape can affect the accuracy of the calculated AAD. For urban aerosol the ultrafine and the lower end of the accumulation mode are dominated by soot particles which is evidenced by the high eBC values in the ultrafine size range. Freshly generated soot particles are complex agglomerates consisting of spherical primary particles with a ca. 40 nm diameter with some additional inner surface area (pores). For those types of particles, the equivalent surface area assumption of spherical particle shape underestimates the actual particle surface area significantly. This agglomerate-structure also reduced the effective mobility density of particles below the corresponding bulk material density, which tends to overpredict the pulmonary dose, if not accounted for properly [43]. Thus, inclusion of soot-specific surface area correction factors for ADD should be explored in the future.

5. Summary and conclusions

A comprehensive mobile air pollution study was conducted in six Lithuanian cities, focusing on the road traffic-related PNSD and eBC. The measurements of PNSD provided a basis for the development of the regional respiratory tract deposition-based pollution impact assessment framework, within which the LUR models were developed for calculated, size-resolved TDSA and ADSA concentrations of airborne particles.

The results showed that urban pollution levels in Lithuania are strongly influenced by a combination of city size, traffic volume, vehicular fleet composition (particularly diesel vehicle percentage), and urban morphology. Vilnius, as the capital and largest city, consistently exhibits the highest concentrations of most pollutants, while Panevėžys shows unexpectedly high pollution levels attributable to its exceptionally high diesel vehicle percentage.

Local factors significantly modify pollution patterns. Klaipėda's coastal location facilitates pollutant dispersion while simultaneously introducing resuspended dust and marine aerosol contributions, resulting in distinctive PNSD dominated by coarse particles. Conversely, inland cities with dense street networks and limited ventilation (such as Vilnius and Kaunas, compared to other Lithuanian cities) experience enhanced pollutant accumulation. Particle size distribution patterns reveal that while ultrafine particles dominate numerically across all cities (70–80 % of total particle number), accumulation mode particles contribute most significantly to particle surface area in most cities, except in Klaipėda, where non-combustion related coarse particles play a substantial role.

In a broader sense, despite Lithuania's relatively aged vehicular fleet—characterized by a high diesel vehicle percentage (50–70 %)—median urban and urban background eBC concentrations align closely with European counterparts, including cities in Central and Southern Europe. Notably, on-road measurements captured direct emission plumes, yielding higher mean eBC values (e.g., Vilnius: 3200 ng/m^3; Panevėžys: 3170 ng/m^3) compared to stationary monitoring data. However, deconvoluted urban background eBC levels (330–710 ng/m^3) remain comparable to cities like Bern and Zurich, reflecting effective pollutant dispersion due to Lithuania's lower population density, reduced traffic volumes, and more open urban layouts (compared to more dense European cities).

While LDSA in Lithuanian cities is broadly consistent with European observations, the TDSA values are markedly elevated (compared to available literature) when coarse particles are included in the calculation. Coastal Klaipėda, influenced by sea spray, resuspended road dust, and port activities, exhibited TDSA concentrations 8–18 times higher than European medians, underscoring the critical role of coarse particles in regional air quality. Similarly, Kaunas' coarse particle burden linked to road construction dust highlights the necessity of multi-modal pollution assessments for health risk evaluations.

Lithuania's recent introduction of limited green zones in Kaunas, aimed at curbing congestion rather than emissions, suggests a pragmatic approach to urban air quality management. Given the country's favorable pollutant dispersion dynamics, tailored strategies—such as controlled vehicle access zones rather than blanket diesel bans—could mitigate localized emissions without compromising mobility. These findings emphasize that while direct emission spikes near traffic sources are significant, background concentrations remain manageable, supporting targeted mitigation measures over broad restrictive policies.

6. Environmental implication

By integrating high-resolution particle size distribution and black carbon measurements with respiratory tract deposition, our study advances environmental exposure assessment by quantifying lung-deposited particle surface area under realistic urban conditions. Identification of spatial and temporal hotspots—driven by coarse dust resuspension in port cities and elevated ultrafine fractions near diesel fleets—enables policymakers to target emission sources more precisely. Transitioning from mass- to deposition-based metrics improves relevance for health risk evaluations and supports region-specific mitigation strategies. Implementing such integrated assessments can guide efficient allocation of control measures, effectively and sustainably reducing population-level exposure to hazardous airborne contaminants in urban environments.

CRediT authorship contribution statement

Manuel J. Jiménez-Navarro: Writing – review & editing, Software. **Manuel Carranza-García:** Writing – review & editing, Software. **Valentino Petrić:** Writing – review & editing, Software. **Mario Lovrić:** Writing – review & editing, Software. **Simonas Kecorius:** Writing – review & editing, Writing – original draft, Visualization, Validation, Supervision, Software, Resources, Project administration, Methodology, Investigation, Funding acquisition, Formal analysis, Data curation, Conceptualization. **del Mar Martínez-Ballesteros María:** Writing – review & editing, Software. **Leizel Madueño:** Writing – review & editing. **Otmar Schmid:** Writing – review & editing. **Magdalena Weiss:** Writing – review & editing. **Steigvilė Byčenkienė:** Writing – review & editing, Supervision, Project administration, Funding acquisition. **Kristina Plauškaitė:** Writing – review & editing, Supervision, Project administration, Funding acquisition. **Gaudentas Kecorius:** Writing – review & editing, Data curation. **Jakob Löndahl:** Writing – review & editing. **Annette Peters:** Writing – review & editing. **Wolfram Birmili:** Writing – review & editing. **Josef Cyrys:** Writing – review & editing.

Declaration of competing interest

The authors declare that they have no known competing financial interests or personal relationships that could have appeared to influence the work reported in this paper.

Acknowledgements

Authors acknowledges funding by the Research Council of Lithuania (LMTLT), agreement No. S-MIP-22–57. ML received funding from the European Commission, grants URBREATH (grant number: 101139711) and Next Generation EU, grant number IA-INT-2024-BioAntroPoP. We sincerely thank the four anonymous reviewers for their constructive and insightful comments, which have significantly contributed to improving the quality of the manuscript.

Appendix A. Supporting information

Supplementary data associated with this article can be found in the online version at doi:10.1016/j.jhazmat.2025.139725.

Data availability

Data will be made available on request.

References

[1] Babu, S.S., Kompalli, S.K., Moorthy, K.K., 2016. Aerosol number size distributions over a coastal semi urban location: seasonal changes and ultrafine particle bursts. Sci Total Environ 563, 351–365.
[2] Batterman, S.A., Zhang, K., Kononowech, R., 2010. Prediction and analysis of near-road concentrations using a reduced-form emission/dispersion model. Environ Health 9, 1–18.
[3] Beelen, R., Voogt, M., Duyzer, J., Zandveld, P., Hoek, G., 2010. Comparison of the performances of land use regression modelling and dispersion modelling in estimating small-scale variations in long-term air pollution concentrations in a Dutch urban area. Atmos Environ 44 (36), 4614–4621.
[4] Bennett, W.D., Zeman, K.L., Kim, C., 1996. Variability of fine particle deposition in healthy adults: effect of age and gender. Am J Respir Crit care Med 153 (5), 1641–1647.
[5] Bessa, M.J., Brandão, F., Rosário, F., Moreira, L., Reis, A.T., Valdiglesias, V., Laffon, B., Fraga, S., Teixeira, J.P., 2023. Assessing the in vitro toxicity of airborne (nano) particles to the human respiratory system: from basic to advanced models. J Toxicol Environ Health Part B 26 (2), 67–96.
[6] Brown, D.M., Wilson, M.R., MacNee, W., Stone, V., Donaldson, K., 2001. Size-dependent proinflammatory effects of ultrafine polystyrene particles: a role for surface area and oxidative stress in the enhanced activity of ultrafines. Toxicol Appl Pharmacol 175 (3), 191–199.
[7] Byčenkienė, S., Ulevicius, V., Kecorius, S., 2011. Characteristics of black carbon aerosol mass concentration over the east baltic region from two-year measurements. J Environ Monit 13 (4), 1027–1038.
[8] Carslaw, D.C., Ropkins, K., 2012. Openair – r package for air quality data analysis. Environ 938 Model Softw 27, 52–61.
[9] Chen, T., Guestrin, C., 2016. Xgboost: a scalable tree boosting system (August). Proc 22nd acm sigkdd Int Conf Knowl Discov data Min 785–794.
[10] Chiesa, M., Bignotti, L., Finco, A., Marzuoli, R., Gerosa, G., 2019. Size-resolved aerosol fluxes above a broadleaved deciduous forest. Agric Meteorol 279, 107757.
[11] Ching, J., Kajino, M., 2018. Aerosol mixing state matters for particles deposition in human respiratory system. Sci Rep 8, 8864.
[12] Cook, R., Isakov, V., Touma, J.S., Benjey, W., Thurman, J., Kinnee, E., Ensley, D., 2008. Resolving local-scale emissions for modeling air quality near roadways. J Air Waste Manag Assoc 58 (3), 451–461.
[13] Crawford, J., Cohen, D.D., Chambers, S.D., Williams, A.G., Atanacio, A., 2019. Impact of aerosols of sea salt origin in a coastal basin: Sydney, Australia. Atmos Environ 207, 52–62.
[14] Diapouli, E., Fetfatzis, P., Panteliadis, P., Spitieri, C., Gini, M.I., Papagiannis, S., Vasilatou, V., Eleftheriadis, K., 2022. PM2. 5 source apportionment and implications for particle hygroscopicity at an urban background site in Athens, Greece. Atmosphere 13 (10), 1685.
[15] Dijkema, M.B., Gehring, U., van Strien, R.T., Van Der Zee, S.C., Fischer, P., Hoek, G., Brunekreef, B., 2011. A comparison of different approaches to estimate small-scale spatial variation in outdoor NO2 concentrations. Environ Health Perspect 119 (5), 670–675.
[16] EIONET, European Environment Agency Central Data Repository. [Online]. Available at: ⟨https://www.eea.europa.eu⟩ [Accessed: 1 January 2025].
[17] European Union, 2024. EU Directive (EU) 2024/2881 of the European Parliament and of the Council of 23 October 2024 on Ambient Air Quality and Cleaner Air for Europe (Recast). Off. J. Eur. Union.
[18] Feng, L., Shen, H., Zhu, Y., Gao, H., Yao, X., 2017. Insight into generation and evolution of sea-salt aerosols from field measurements in diversified marine and coastal atmospheres. Sci Rep 7 (1), 41260.
[19] Fung, P.L., Zaidan, M.A., Niemi, J.V., Saukko, E., Timonen, H., Kousa, A., Kuula, J., Rönkkö, T., Karppinen, A., Tarkoma, S., Kulmala, M., 2022. Input-adaptive linear mixed-effects model for estimating alveolar lung-deposited surface area (LDSA) using multipollutant datasets. Atmos Chem Phys 22 (3), 1861–1882.
[20] Ganguly, K., Ettehadieh, D., Upadhyay, S., Takenaka, S., Adler, T., Karg, E., Krombach, F., Kreyling, W.G., Schulz, H., Schmid, O., Stoeger, T., 2017. Early pulmonary response is critical for extra-pulmonary carbon nanoparticle mediated effects: comparison of inhalation versus intra-arterial infusion exposures in mice. Part Fibre Toxicol 14, 1–17.
[21] Hagler, G.S., Yelverton, T.L., Vedantham, R., Hansen, A.D., Turner, J.R., 2011. Post-processing method to reduce noise while preserving high time resolution in aethalometer real-time black carbon data. Aerosol Air Qual Res 11 (5), 539–546.
[22] Hänninen, O., Brüske-Hohlfeld, I., Loh, M., Stoeger, T., Kreyling, W., Schmid, O., Peters, A., 2010. Occupational and consumer risk estimates for nanoparticles emitted by laser printers. J Nanopart Res 12, 91–99.
[23] HEI Review Panel on Ultrafine Particles (2013) Understanding the Health Effects of Ambient Ultrafine Particles. HEI Perspectives 3. Boston, MA: Health Effects Institute.
[24] Hennig, F., Quass, U., Hellack, B., Küpper, M., Kuhlbusch, T.A.J., Stafoggia, M., et al., 2018. Ultrafine and fine particle number and surface area concentrations and daily Cause-specific mortality in the ruhr area, Germany, 2009-2014. Environ Health Perspect 126 (2), 027008.
[25] Hennig, F., Sugiri, D., Tzivian, L., Fuks, K., Moebus, S., Jöckel, K.H., Vienneau, D., Kuhlbusch, T.A., De Hoogh, K., Memmesheimer, M., Jakobs, H., 2016. Comparison of land-use regression modeling with dispersion and chemistry transport modeling to assign air pollution concentrations within the ruhr area. Atmosphere 7 (3), 48.
[26] Hosiokangas, J., Vallius, M., Ruuskanen, J., Mirme, A., Pekkanen, J., 2004. Resuspended dust episodes as an urban air-quality problem in subarctic regions. Scand J Work Environ Health 28–35.
[27] Hussain, S., Boland, S., Baeza-Squiban, A., Hamel, R., Thomassen, L.C.J., Martens, J.A., et al., 2009. Oxidative stress and proinflammatory effects of carbon black and titanium dioxide nanoparticles: role of particle surface area and internalized amount. Toxicology 260 (1-3), 142, 9.
[28] Janssen, N.A., Hoek, G., Simic-Lawson, M., Fischer, P., Van Bree, L., Ten Brink, H., Keuken, M., Atkinson, R.W., Anderson, H.R., Brunekreef, B., Cassee, F.R., 2011. Black carbon as an additional indicator of the adverse health effects of airborne particles compared with PM10 and PM2. 5. Environ Health Perspect 119 (12), 1691–1699.
[29] Järvinen, A., Aitomaa, M., Rostedt, A., Keskinen, J., Yli-Ojanperä, J., 2014. Calibration of the new electrical low pressure impactor (ELPI+). J Aerosol Sci 69, 150–159.
[30] Kecorius, S., Madueño, L., Sues, S., Cyrys, J., Lovrić, M., Pöhlker, M., Plauškaitė, K., Davulienė, L., Minderytė, A., Byčenkienė, S., 2024. Development of a cost-effective adsorption dryer for high-quality aerosol sampling. Aerosol Air Qual Res 24 (3), 230057.
[31] Kecorius, S., Madueño, L., Vallar, E., Alas, H., Betito, G., Birmili, W., Cambaliza, M. O., Catipay, G., Gonzaga-Cayetano, M., Galvez, M.C., Lorenzo, G., 2017. Aerosol particle mixing state, refractory particle number size distributions and emission factors in a polluted urban environment: case study of metro Manila, Philippines. Atmos Environ 170, 169–183.
[32] Kecorius, S., Sues, S., Madueño, L., Wiedensohler, A., Winkler, U., Held, A., Lüchtrath, S., Beddows, D.C., Harrison, R.M., Lovric, M., Soppa, V., 2024. Aerosol particle number concentration, ultrafine particle number fraction, and new particle formation measurements near the international airports in Berlin, Germany–First results from the BEAR study. Environ Int 193, 109086.
[33] Kim, C.S., Hu, S.C., Jacques, P., 2002. Analysis of respiratory deposition of inhaled particles for different dose metrics: comparison of number, surface area and mass dose of typical ambient bi-modal aerosols. Presente Am Thorac Soc Meet.
[34] Kivekäs, N., Massling, A., Grythe, H., Lange, R., Rusnak, V., Carreno, S., Skov, H., Swietlicki, E., Nguyen, Q.T., Glasius, M., Kristensson, A., 2014. Contribution of ship traffic to aerosol particle concentrations downwind of a major shipping lane. Atmos Chem Phys 14 (16), 8255–8267.
[35] Koehler, K.A., Kreidenweis, S.M., DeMott, P.J., Petters, M.D., Prenni, A.J., Carrico, C.M., 2009. Hygroscopicity and cloud droplet activation of mineral dust aerosol. Geophys Res Lett 36 (8).
[36] Lepistö, T., Lintusaari, H., Oudin, A., Barreira, L.M., Niemi, J.V., Karjalainen, P., Salo, L., Silvonen, V., Markkula, L., Hoivala, J., Marjanen, P., 2023. Particle lung deposited surface area (LDSAal) size distributions in different urban environments and geographical regions: towards understanding of the PM2. 5 dose–response. Environ Int 180, 108224.
[37] Levy, J.I., Hanna, S.R., 2011. Spatial and temporal variability in urban fine particulate matter concentrations. Environ Pollut 159 (8-9), 2009–2015.
[38] LHS, Lithuanian Hydrometeorological Service. [Online]. Available at: ⟨https://www.meteo.lt⟩ [Accessed: 1 January 2025].
[39] Li, G., Lu, P., Deng, S., Gao, J., Lu, Z., Li, Q., 2023. Spatial variability and health assessment of particle number concentration at different exposure locations near urban traffic arterial: a case study in xi'an, China. Atmos Environ 314, 120086.
[40] Linell, J., Isaxon, C., Olsson, B., Stroh, E., Wollmer, P., Löndahl, J., Rissler, J., 2024. Effects of breathing variables on modelled particle lung deposition at physical activity for children and adults. Air quality. Atmosphere Health 17 (4), 843–856.
[41] Liu, X., Hadiatullah, H., Zhang, X., Hill, L.D., White, A.H., Schnelle-Kreis, J., Bendl, J., Jakobi, G., Schloter-Hai, B., Zimmermann, R., 2021. Analysis of mobile monitoring data from the microAeth® MA200 for measuring changes in black carbon on the roadside in augsburg. Atmos Meas Tech Discuss 2021, 1–18.
[42] Liu, X., Hadiatullah, H., Zhang, X., Trechera, P., Savadkoohi, M., Garcia-Marlès, M., Reche, C., Pérez, N., Beddows, D.C., Salma, I., Thén, W., 2023. Ambient air particulate total lung deposited surface area (LDSA) levels in urban Europe. Sci Total Environ 898, 165466.

[43] Lizonova, D., Nagarkar, A., Demokritou, P., Kelesidis, G.A., 2024. Effective density of inhaled environmental and engineered nanoparticles and its impact on the lung deposition and dosimetry. Part Fibre Toxicol 21 (1), 7.
[44] Löndahl, J., Möller, W., Pagels, J.H., Kreyling, W.G., Swietlicki, E., Schmid, O., 2014. Measurement techniques for respiratory tract deposition of airborne nanoparticles: a critical review. J Aerosol Med Pulm Drug Deliv 27 (4), 229–254.
[45] LSIP, Lithuanian Spatial Information Portal. [Online]. Available at: ⟨https://www.geoportal.lt⟩ [Accessed: 1 January 2025].
[46] Ma, X., Zou, B., Deng, J., Gao, J., Longley, I., Xiao, S., Guo, B., Wu, Y., Xu, T., Xu, X., Yang, X., 2024. A comprehensive review of the development of land use regression approaches for modeling spatiotemporal variations of ambient air pollution: a perspective from 2011 to 2023. Environ Int 183, 108430.
[47] Man, R., Wu, Z., Zong, T., Voliotis, A., Qiu, Y., Größ, J., van Pinxteren, D., Zeng, L., Herrmann, H., Wiedensohler, A., Hu, M., 2022. Impact of water uptake and mixing state on submicron particle deposition in the human respiratory tract (HRT) based on explicit hygroscopicity measurements at HRT-like conditions. Atmos Chem Phys 22 (18), 12387–12399.
[48] McMurray, R.G., Ahlborn, S.W., 1982. Respiratory responses to running and walking at the same metabolic rate. Respir Physiol 47 (2), 257–265.
[49] Ohlwein, S., Kappeler, R., Kutlar Joss, M., Künzli, N., Hoffmann, B., 2019. Health effects of ultrafine particles: a systematic literature review update of epidemiological evidence. Int J Public Health 64, 547–559.
[50] OSM, Open Street Map services. [Online]. Available at: ⟨https://www.geofabrik.de⟩ [Accessed: 1 January 2025].
[51] Ostro, B., Tobias, A., Karanasiou, A., Samoli, E., Querol, X., Rodopoulou, S., Basagaña, X., Eleftheriadis, K., Diapouli, E., Vratolis, S., Jacquemin, B., 2015. The risks of acute exposure to black carbon in Southern Europe: results from the MED-PARTICLES project. Occup Environ Med 72 (2), 123–129.
[52] Peters, A., Veronesi, B., Calderón-Garcidueñas, L., Gehr, P., Chen, L.C., Geiser, M., Reed, W., Rothen-Rutishauser, B., Schürch, S., Schulz, H., 2006. Translocation and potential neurological effects of fine and ultrafine particles a critical update. Part Fibre Toxicol 3 (1), 13.
[53] Price, H.D., Stahlmecke, B., Arthur, R., Kaminski, H., Lindermann, J., Däuber, E., Asbach, C., Kuhlbusch, T.A., Berube, K.A., Jones, T.P., 2014. Comparison of instruments for particle number size distribution measurements in air quality monitoring. J Aerosol Sci 76, 48–55.
[54] QGIS Development Team. 2022. QGIS Geographic Information System. Open Source Geospatial Foundation Project. [Online]. Available at: ⟨https://qgis.org⟩ [Accessed: 1 January 2025].
[55] QtiPlot. 2008. QtiPlot: Data analysis and scientific visualization [Online]. Available at: ⟨https://www.qtiplot.com/⟩ [Accessed: 3 April 2023].
[56] R Core Team. R: A language and environment for statistical computing. R Foundation for Statistical Computing; Vienna, Austria: 2013.
[57] Regitra. [Online]. Available at: ⟨https://www.regitra.lt/lt/atviri-duomenys⟩ [Accessed: 1 January 2025].
[58] Rienda, I.C., Nunes, T., Gonçalves, C., Vicente, A., Amato, F., Lucarelli, F., Kováts, N., Hubai, K., Sainnokhoi, T.A., Alves, C.A., 2023. Road dust resuspension in a coastal atlantic intermunicipal urban area with industrial facilities: emission factors, chemical composition and ecotoxicity. Atmos Res 294, 106977.
[59] Rose, C., Collaud Coen, M., Andrews, E., Lin, Y., Bossert, I., Lund Myhre, C., Tuch, T., Wiedensohler, A., Fiebig, M., Aalto, P., Alastuey, A., 2021. Seasonality of the particle number concentration and size distribution: a global analysis retrieved from the network of global atmosphere watch (GAW) near-surface observatories. Atmos Chem Phys Discuss 2021, 1–69.
[60] Sartelet, K., Kerckhoffs, J., Athanasopoulou, E., Lugon, L., Vasilescu, J., Zhong, J., Hoek, G., Joly, C., Park, S.J., Talianu, C., van den Elshout, S., 2025. Air pollution mapping and variability over five european cities. Environ Int 199, 109474.
[61] Savadkoohi, M., Pandolfi, M., Reche, C., Niemi, J.V., Mooibroek, D., Titos, G., Green, D.C., Tremper, A.H., Hueglin, C., Liakakou, E., Mihalopoulos, N., 2023. The variability of mass concentrations and source apportionment analysis of equivalent black carbon across urban Europe. Environ Int 178, 108081.
[62] Schmid, O., Cassee, F.R., 2017. On the pivotal role of dose for particle toxicology and risk assessment: exposure is a poor surrogate for delivered dose. Part Fibre Toxicol 14, 1–5.
[63] Schmid, O., Möller, W., Semmler-Behnke, M., A. Ferron, G., Karg, E., Lipka, J., Schulz, H., Kreyling, W.G., Stöger, T., 2009. Dosimetry and toxicology of inhaled ultrafine particles. Biomarkers 14 (sup1), 67–73.
[64] Schmid, O., Stoeger, T., 2016. Surface area is the biologically most effective dose metric for acute nanoparticle toxicity in the lung. J Aerosol Sci 99, 133–143.
[65] Schwarz, M., Schneider, A., Cyrys, J., Bastian, S., Breitner, S., Peters, A., 2023. Impact of ultrafine particles and total particle number concentration on five cause-specific hospital admission endpoints in three German cities. Environ Int 178, 108032.
[66] SECR, State Enterprise Centre of Registers. [Online]. Available at: ⟨https://www.registrucentras.lt⟩ [Accessed: 1 January 2025].
[67] Silvonen, V., Salo, L., Raunima, T., Vojtisek-Lom, M., Ondracek, J., Topinka, J., Schins, R.P., Lepistö, T., Lintusaari, H., Saarikoski, S., Barreira, L.M., 2023. Lung-depositing surface area (LDSA) of particles in office spaces around Europe: size distributions, I/O-ratios and infiltration. Build Environ 246, 110999.
[68] Smith, H., 1994. Human respiratory tract model for radiological protection. ICRP Publ 66.
[69] Stoeger, T., Takenaka, S., Frankenberger, B., Ritter, B., Karg, E., Maier, K., Schulz, H., Schmid, O., 2009. Deducing in vivo toxicity of combustion-derived nanoparticles from a cell-free oxidative potency assay and metabolic activation of organic compounds. Environ Health Perspect 117 (1), 54–60.
[70] Valavanidis, A., Fiotakis, K., Vlachogianni, T., 2008. Airborne particulate matter and human health: toxicological assessment and importance of size and composition of particles for oxidative damage and carcinogenic mechanisms. J Environ Sci Health Part C 26 (4), 339–362.
[71] Vallabani, N.S., Gruzieva, O., Elihn, K., Juárez-Facio, A.T., Steimer, S.S., Kuhn, J., Silvergren, S., Portugal, J., Piña, B., Olofsson, U., Johansson, C., 2023. Toxicity and health effects of ultrafine particles: towards an understanding of the relative impacts of different transport modes. Environ Res 231, 116186.
[72] Vilcassim, R., Thurston, G.D., 2023. Gaps and future directions in research on health effects of air pollution. EBioMedicine 93.
[73] von der Weiden, S.-L., Drewnick, F., and Borrmann, S. n.d. Particle Loss Calculator – a new software tool for the assessment of the performance of aerosol inlet systems, Atmos. Meas. Tech., 2, 479–494.
[74] Vu, T.V., Shi, Z., Harrison, R.M., 2021. Estimation of hygroscopic growth properties of source-related sub-micrometre particle types in a mixed urban aerosol. npj Clim Atmos Sci 4 (1), 21.
[75] Wickham, H., 2011. ggplot2. Wiley Interdiscip Rev Comput Stat 3 (2), 180–185.
[76] World Health Organization, 2021. WHO global air quality guidelines: particulate matter (PM2.5 and PM10), ozone, nitrogen dioxide, sulfur dioxide and carbon monoxide. World Health Organization.